Full Parameter Estimation for Permanent Magnet Synchronous Motors

Yelong Yu ⓘ, Xiaoyan Huang ⓘ, *Member, IEEE*, Zhaokai Li ⓘ, Min Wu ⓘ, Tingna Shi ⓘ, *Member, IEEE*, Yanfei Cao ⓘ, Geng Yang ⓘ, *Member, IEEE*, and Feng Niu ⓘ, *Member, IEEE*

Abstract—**This article elaborates a novel online full parameter estimation method for permanent magnet synchronous motors (PMSMs). Usually, only two parameters can be estimated using voltage functions in the *d-q* frame due to the problem of rank deficiency. The α-β frame possesses the inherent advantage that full motor parameters can be estimated using voltage functions during steady and transient states. An algorithm based on recursive least squares in the α-β frame is proposed to estimate full motor parameters, including stator resistance, *d*-axis and *q*-axis inductances, and flux linkage simultaneously. Simulation and experimental results on the PMSM drive system are presented to verify the effectiveness of the proposed algorithm. Compared with the method in the *d-q* frame, the superiority of the proposed method in terms of faster convergence rate, less computational cost, and high accuracy is demonstrated.**

Index Terms—**Full parameter estimation, permanent magnet synchronous motors (PMSMs), recursive least squares (RLS).**

I. INTRODUCTION

THERE are many distinguishing characteristics of permanent magnet synchronous motors (PMSMs) such as wide speed range, high power density, and high efficiency [1]; hence, PMSMs are employed in many applications. For the control of PMSMs, getting the knowledge of motor electrical parameters, including stator resistance, rotor flux linkage, and *d*-axis and *q*-axis inductances, is extremely crucial especially in some situations that the parameters diverge from their nominal values [2],

[3]. The methods of estimating parameters can be divided into offline and online ones. The offline estimation methods rely on the offline measurements of motor parameters [4], [5]. Apart from offline methods, the online approaches are able to estimate full parameters in real time: an adaptive online parameter estimation is introduced in [6]; a current loop parameter estimation based on the Bode diagram is demonstrated in [7]; and some self-learning techniques such as neural network [8], flower pollination algorithm [9], and genetic algorithm [10] are studied to accomplish the parameter estimation.

Most online estimation methods in the literature are conducted in the *d-q* frame. According to the voltage functions in the *d-q* frame, the rank of observability matrix is 2 in the steady state [11], [12], which is less than the number of full parameters to be estimated (there are four parameters mentioned above). Usually, one motor parameter can be identified using each of the voltage functions in the *d-q* frame, which means only two parameters can be estimated in total using the *d-q* voltage functions once. The comprehensive study in [13] points out that the problem of rank deficiency in the *d-q* frame is a major concern in parameter estimation; the estimation results may not converge to the correct values. Approaches are presented to overcome the problem of rank deficiency in the *d-q* frame [14]–[23], most of them are dependent on two basic principles: one is to decrease the number of parameters to be estimated, and the other is to increase the rank of observability matrix.

To decrease parameters, some motor parameters have to be fixed via offline measurement results or neglected for their small proportion. For instance, in [14], the values of rotor flux linkage, and *d*-axis and *q*-axis inductances are fixed to solely estimate the stator resistance for sensorless control. The inductance is ignored since the item of pLi occupies very small proportion in voltage [15]. The accuracy of estimated parameters is subject to the variations of those fixed parameters by using this method. In [16], two separate estimation algorithms are designed with fast and slow convergence rate: the first one is utilized to estimate only two fast time-varying parameters (*d*-axis and *q*-axis inductances), while the second algorithm is used to identify the other two slow time-varying parameters (stator resistance and rotor flux linkage). However, the method in [16] has to use the affine projection algorithms for four times to estimate full parameters.

To increase the rank, a popular technique is signal injection. In [17], pseudorandom signals such as M-sequence signals were superimposed upon *d*-axis and *q*-axis currents, which need a large amplitude up to 6% of rated current. High-frequency square

wave voltage is injected to estimate inductance in [18]. The injected harmonic current [19] and measured speed harmonics [20] are used to obtain the knowledge of magnet flux linkage. Choi [21] utilized the stator current ripples in the *d-q* frame to achieve the real-time estimation of full parameters. In addition, by setting different values of *d*-axis stator current in the steady stage, the algorithm in [22] could identify the full parameters at the same time. Interestingly, position angle offset is added to increase the voltage functions in [23]. However, the methods above changed the operating state or working point of motors, which would cause parameter variations and lead to estimation errors.

Considering the limitations in the *d-q* frame, this article moves to the stationary frame to accomplish the full parameter estimation. To simplify the algorithms, the α-β stationary frame is adopted in this article. The α-β frame possesses the inherent advantage that two motor parameters can be estimated using each of the voltage functions. With two voltage functions in the α-β frame, full motor parameters can be estimated during both steady and transient states. Then, a full parameter estimation algorithm for the PMSM in the α-β frame is proposed. In Section II, parameter observability is first analyzed since it is often regarded as the big concern for parameter estimation. With the help of recursive least squares (RLS), a full parameter estimation algorithm in the α-β frame is designed in Section III. At the end of this article, simulations based on MATLAB/Simulink and experiments on the PMSM drive system with a microcontroller of STM32F103 are presented to verify the effectiveness of the proposed algorithm during steady and transient states. Moreover, a contrastive study with the conventional methods in the *d-q* frame and other existing methods such as Kalman filter is carried out to prove the superiority of the proposed method, such as faster convergence rate, less usage of RLS algorithms, and less computational cost.

II. PMSM MODEL AND PARAMETER OBSERVABILITY

A. PMSM Model in the d-q Frame

The mathematical model of the PMSM in rotating *d-q* frame can be expressed as

$$
\begin{aligned}
v_d &= R_s i_d + p L_d i_d - \omega_e L_q i_q \\
v_q &= R_s i_q + p L_q i_q + \omega_e L_d i_d + \omega_e \psi_f
\end{aligned} \quad (1)
$$

where v_d and v_q are the voltages in the *d-q* frame, i_d and i_q are the currents in the *d-q* frame, R_s, L_d, and L_q represent the stator resistance, *d*-axis stator inductance, and *q*-axis stator inductance, respectively, ω_e is the electrical angular velocity, ψ_f is the flux linkage, and p is the derivative symbol.

B. PMSM Model in the α-β Frame

The transformation from the *d-q* frame to the α-β frame can be expressed as

$$
\begin{bmatrix} F_\alpha \\ F_\beta \end{bmatrix} = \begin{bmatrix} \cos\theta_e & -\sin\theta_e \\ \sin\theta_e & \cos\theta_e \end{bmatrix} \begin{bmatrix} F_d \\ F_q \end{bmatrix} \quad (2)
$$

where F refers to voltage or current and θ_e is the electrical angle of rotor position. Then, the mathematical model of the PMSM in the $\alpha\beta$ frame can be deduced from (1) and (2) as

$$
\begin{bmatrix} v_\alpha \\ v_\beta \end{bmatrix} = \begin{bmatrix} R_s + p L_d & \omega_e(L_d - L_q) \\ -\omega_e(L_d - L_q) & R_s + p L_d \end{bmatrix} \begin{bmatrix} i_\alpha \\ i_\beta \end{bmatrix}
$$
$$
+ \left[(L_d - L_q)(\omega_e i_d - p i_q) + \omega_e \psi_f \right] \begin{bmatrix} -\sin\theta_e \\ \cos\theta_e \end{bmatrix} \quad (3)
$$

where v_α and v_β are the voltages in the $\alpha\beta$ frame and i_α and i_β are the currents in the α-β frame. It should be noted that, in general, the inductances to be estimated are *d*-axis and *q*-axis inductances. Thus, in the model (3), L_d and L_q are used rather than the α-axis inductance L_α and β-axis inductance L_β.

C. Parameter Observability Theory

Before the procedure of parameter estimation, the observability should be first analyzed; the theory of parameter observability is depicted in [24] and [25]. For a given dynamic system, we have

$$
\frac{d}{dt}\boldsymbol{x} = \boldsymbol{f}(\boldsymbol{x}, \boldsymbol{u}), \boldsymbol{y} = \boldsymbol{h}(\boldsymbol{x}) \quad (4)
$$

where $\boldsymbol{x} \in \mathrm{R}^n$ is the vector of state variables, $\boldsymbol{u} \in \mathrm{R}^m$ is the input vector, $\boldsymbol{y}$ is the output vector, and $\boldsymbol{f}$ and $\boldsymbol{h}$ are the state and output functions, respectively. By virtue of observability theory in [26], the vector of state variables $\boldsymbol{x}$ in (4) can be observable if the matrix $\boldsymbol{O}$ is full-rank, which is described as

$$
\mathrm{rank}(\boldsymbol{O}) = n \quad (5)
$$

where O is the Jacobian matrix of L

$$
\boldsymbol{O} = \frac{\partial \boldsymbol{L}}{\partial \boldsymbol{x}}, \boldsymbol{L} = \begin{bmatrix} \mathcal{L}_f^0 \boldsymbol{h} & \mathcal{L}_f^1 \boldsymbol{h} \dots \mathcal{L}_f^{n-1} \boldsymbol{h} \end{bmatrix}^T . \quad (6)
$$

$\mathcal{L}_f^k \boldsymbol{h}$ refers to the *k*th-order Lie derivative of output function $\boldsymbol{h}$, and there are

$$
\mathcal{L}_f^0 \boldsymbol{h} = \boldsymbol{h}, \mathcal{L}_f^1 \boldsymbol{h} = (\bigtriangledown \boldsymbol{h})\boldsymbol{f} = \frac{\partial \boldsymbol{h}}{\partial \boldsymbol{x}}\boldsymbol{f} = \sum_{i=1}^{n} \frac{\partial \boldsymbol{h}}{\partial x_i} f_i
$$
$$
\mathcal{L}_f^k \boldsymbol{h} = \mathcal{L}_f \mathcal{L}_f^{k-1} \boldsymbol{h}. \quad (7)
$$

D. Parameter Observability in the d-q Frame

The parameter observability theory above is used to analyze the observability of state variables. In order to figure out the observability of motor parameters in the *d-q* frame, the vector of state variables should be extended to motor parameters. Assuming that all of the motor parameters are constant within a short time, from (1), we have

$$
\frac{d}{dt} i_d = \frac{-R_s}{L_d} i_d + \omega_e \frac{L_q}{L_d} i_q + \frac{1}{L_d} v_d
$$
$$
\frac{d}{dt} i_q = \frac{-R_s}{L_q} i_q - \omega_e \frac{L_d}{L_q} i_d + \frac{1}{L_q}(v_q - \omega_e \psi_f)
$$
$$
\frac{d}{dt} R_s = 0; \frac{d}{dt} L_d = 0; \frac{d}{dt} L_q = 0; \frac{d}{dt} \psi_f = 0. \quad (8)
$$

Let

$$
\boldsymbol{x} = \begin{bmatrix} i_d i_q R_s L_d L_q \psi_f \end{bmatrix}^T, \boldsymbol{y} = \boldsymbol{h}(\boldsymbol{x}) = \begin{bmatrix} i_d i_q \end{bmatrix}^T
$$

$$\boldsymbol{u} = \begin{bmatrix} v_d v_q \omega_e \end{bmatrix}^T \tag{9}$$

$$\boldsymbol{f}(\boldsymbol{x}, \boldsymbol{u}) = \begin{bmatrix} \frac{-R_s}{L_d} i_d + \omega_e \frac{L_q}{L_d} i_q + \frac{1}{L_d} v_d \\ \frac{-R_s}{L_q} i_q - \omega_e \frac{L_d}{L_q} i_d + \frac{1}{L_q} (v_q - \omega_e \psi_f) \\ 0 \\ 0 \\ 0 \\ 0 \end{bmatrix}. \tag{10}$$

According to (7), (9), and (10), the Lie derivative of output function $\boldsymbol{h}$ can be described as

$$\mathcal{L}_f^0 \boldsymbol{h} = \boldsymbol{h} = \begin{bmatrix} i_d i_q \end{bmatrix}^T$$

$$\mathcal{L}_f^1 \boldsymbol{h} = (\bigtriangledown \boldsymbol{h}) \boldsymbol{f} = \begin{bmatrix} \frac{d}{dt} i_d \frac{d}{dt} i_q \end{bmatrix}^T$$

$$\mathcal{L}_f^2 \boldsymbol{h} = (\bigtriangledown \mathcal{L}_f^1 \boldsymbol{h}) \boldsymbol{f} = \boldsymbol{A} \begin{bmatrix} \frac{d}{dt} i_d \frac{d}{dt} i_q \end{bmatrix}^T$$

$$\mathcal{L}_f^3 \boldsymbol{h} = (\bigtriangledown \mathcal{L}_f^2 \boldsymbol{h}) \boldsymbol{f} = \boldsymbol{A}^2 \begin{bmatrix} \frac{d}{dt} i_d \frac{d}{dt} i_q \end{bmatrix}^T$$

$$\mathcal{L}_f^4 \boldsymbol{h} = (\bigtriangledown \mathcal{L}_f^3 \boldsymbol{h}) \boldsymbol{f} = \boldsymbol{A}^3 \begin{bmatrix} \frac{d}{dt} i_d \frac{d}{dt} i_q \end{bmatrix}^T$$

$$\mathcal{L}_f^5 \boldsymbol{h} = (\bigtriangledown \mathcal{L}_f^4 \boldsymbol{h}) \boldsymbol{f} = \boldsymbol{A}^4 \begin{bmatrix} \frac{d}{dt} i_d \frac{d}{dt} i_q \end{bmatrix}^T \tag{11}$$

where

$$\boldsymbol{A} = \begin{bmatrix} \frac{-R_s}{L_d} & \omega_e \frac{L_q}{L_d} \\ -\omega_e \frac{L_d}{L_q} & \frac{-R_s}{L_q} \end{bmatrix}. \tag{12}$$

Then, the elements of observability matrix $\boldsymbol{O}$ can be calculated as

$$\frac{\partial \mathcal{L}_f^2 \boldsymbol{h}}{\partial \boldsymbol{x}} = \frac{\partial \boldsymbol{A}}{\partial \boldsymbol{x}} \begin{bmatrix} \frac{d}{dt} i_d \frac{d}{dt} i_q \end{bmatrix}^T + \boldsymbol{A} \frac{\partial \mathcal{L}_f^1 \boldsymbol{h}}{\partial \boldsymbol{x}}$$

$$\frac{\partial \mathcal{L}_f^3 \boldsymbol{h}}{\partial \boldsymbol{x}} = 2\boldsymbol{A} \frac{\partial \boldsymbol{A}}{\partial \boldsymbol{x}} \begin{bmatrix} \frac{d}{dt} i_d \frac{d}{dt} i_q \end{bmatrix}^T + \boldsymbol{A}^2 \frac{\partial \mathcal{L}_f^1 \boldsymbol{h}}{\partial \boldsymbol{x}}$$

$$= 2\boldsymbol{A} \left(\frac{\partial \boldsymbol{A}}{\partial \boldsymbol{x}} \begin{bmatrix} \frac{d}{dt} i_d \frac{d}{dt} i_q \end{bmatrix}^T + \boldsymbol{A} \frac{\partial \mathcal{L}_f^1 \boldsymbol{h}}{\partial \boldsymbol{x}} \right) - \boldsymbol{A}^2 \frac{\partial \mathcal{L}_f^1 \boldsymbol{h}}{\partial \boldsymbol{x}}$$

$$= 2\boldsymbol{A} \frac{\partial \mathcal{L}_f^2 \boldsymbol{h}}{\partial \boldsymbol{x}} - \boldsymbol{A}^2 \frac{\partial \mathcal{L}_f^1 \boldsymbol{h}}{\partial \boldsymbol{x}}$$

$$\frac{\partial \mathcal{L}_f^4 \boldsymbol{h}}{\partial \boldsymbol{x}} = 3\boldsymbol{A}^2 \frac{\partial \mathcal{L}_f^2 \boldsymbol{h}}{\partial \boldsymbol{x}} - 2\boldsymbol{A}^3 \frac{\partial \mathcal{L}_f^1 \boldsymbol{h}}{\partial \boldsymbol{x}}$$

$$\frac{\partial \mathcal{L}_f^5 \boldsymbol{h}}{\partial \boldsymbol{x}} = 4\boldsymbol{A}^3 \frac{\partial \mathcal{L}_f^2 \boldsymbol{h}}{\partial \boldsymbol{x}} - 3\boldsymbol{A}^4 \frac{\partial \mathcal{L}_f^1 \boldsymbol{h}}{\partial \boldsymbol{x}}. \tag{13}$$

It can be seen that the rank of matrix O depends on the rank of $[\frac{\partial \mathcal{L}_f^1 \boldsymbol{h}}{\partial \boldsymbol{x}} \frac{\partial \mathcal{L}_f^2 \boldsymbol{h}}{\partial \boldsymbol{x}}]^T$, which means $\frac{\partial \mathcal{L}_f^3 \boldsymbol{h}}{\partial \boldsymbol{x}}, \frac{\partial \mathcal{L}_f^4 \boldsymbol{h}}{\partial \boldsymbol{x}}$, and $\frac{\partial \mathcal{L}_f^5 \boldsymbol{h}}{\partial \boldsymbol{x}}$ can be ignored when analyzing the rank of matrix O. Additionally, considering the fact that i_d and i_q can be calculated from measured phase currents of motor, there is no need to estimate them. Therefore, the submatrix $\boldsymbol{O}_{\text{sub}}$ from O can be used to analyze the observability

$$\boldsymbol{O}_{\text{sub}} = \begin{bmatrix} \frac{\partial \mathcal{L}_f^1 h_1}{\partial R_s} & \frac{\partial \mathcal{L}_f^1 h_1}{\partial L_d} & \frac{\partial \mathcal{L}_f^1 h_1}{\partial L_q} & \frac{\partial \mathcal{L}_f^1 h_1}{\partial \psi_f} \\ \frac{\partial \mathcal{L}_f^1 h_2}{\partial R_s} & \frac{\partial \mathcal{L}_f^1 h_2}{\partial L_d} & \frac{\partial \mathcal{L}_f^1 h_2}{\partial L_q} & \frac{\partial \mathcal{L}_f^1 h_2}{\partial \psi_f} \\ \frac{\partial \mathcal{L}_f^2 h_1}{\partial R_s} & \frac{\partial \mathcal{L}_f^2 h_1}{\partial L_d} & \frac{\partial \mathcal{L}_f^2 h_1}{\partial L_q} & \frac{\partial \mathcal{L}_f^2 h_1}{\partial \psi_f} \\ \frac{\partial \mathcal{L}_f^2 h_2}{\partial R_s} & \frac{\partial \mathcal{L}_f^2 h_2}{\partial L_d} & \frac{\partial \mathcal{L}_f^2 h_2}{\partial L_q} & \frac{\partial \mathcal{L}_f^2 h_2}{\partial \psi_f} \end{bmatrix}$$

$$= \begin{bmatrix} -\frac{1}{L_d} i_d & -\frac{1}{L_d} \frac{di_d}{dt} & \frac{1}{L_d} i_q \omega_e & 0 \\ -\frac{1}{L_q} i_q & -\frac{1}{L_q} i_d \omega_e & -\frac{1}{L_q} \frac{di_q}{dt} & -\frac{1}{L_q} \omega_e \\ \frac{R_s i_d - \omega_e L_d i_q - L_d \frac{di_d}{dt}}{L_d{}^2} & \frac{O_{32}}{L_d{}^2} & -\frac{R_s \omega_e i_q}{L_d{}^2} & -\frac{\omega_e{}^2 L_d}{L_d{}^2} \\ \frac{R_s i_q + \omega_e L_q i_d + L_q \frac{di_q}{dt}}{L_q{}^2} & \frac{R_s \omega_e i_d}{L_q{}^2} & \frac{O_{43}}{L_q{}^2} & \frac{R_s \omega_e}{L_q{}^2} \end{bmatrix} \tag{14}$$

where

$$O_{32} = \omega_e L_d \frac{di_q}{dt} - \omega_e{}^2 L_d i_d + 2R_s \frac{di_d}{dt}$$

$$O_{43} = \omega_e L_q \frac{di_d}{dt} - \omega_e{}^2 L_q i_q - 2R_s \frac{di_q}{dt}. \tag{15}$$

In the transient state when i_d and i_q differ from previous values, their derivatives are not zero. Given a specific nonzero speed ω_e, it can be seen from (14) and (15) that in the transient state, the motor parameters are fully observable because the matrix in (14) is full-rank. However, when it comes to the steady state, the derivatives of i_d and i_q are regarded as zero

$$\frac{di_d}{dt} = 0, \frac{di_q}{dt} = 0. \tag{16}$$

Thus, in the steady state, the rank of observability matrix $\boldsymbol{O}'_{\text{sub}}$ becomes (some items in $\boldsymbol{O}_{\text{sub}}$ are deleted since the primary row transformation has no impact on the matrix rank)

$$\text{rank}(\boldsymbol{O}'_{\text{sub}}) =$$

$$\text{rank} \begin{bmatrix} -i_d & 0 & i_q \omega_e & 0 \\ -i_q & -i_d \omega_e & 0 & -\omega_e \\ R_s i_d - \omega_e L_d i_q & -\omega_e{}^2 L_d i_d & -R_s \omega_e i_q & -\omega_e{}^2 L_d \\ R_s i_q + \omega_e L_q i_d & R_s \omega_e i_d & -\omega_e{}^2 L_q i_q & R_s \omega_e \end{bmatrix}. \tag{17}$$

It can be found that $\boldsymbol{O}'_{\text{sub}}$ is not full-rank because the second column and the fourth are linearly dependent [27]. Now, it is clear that in the steady state, the parameters are not fully observable on the account of rank deficiency in the d-q frame. In the transient state, the parameters can be fully observable. It should be remarked that the d-q frame plays a prominent role in the vector control of PMSMs. However, it is not the best choice for full parameter estimation.

E. Parameter Observability in the α-β Frame

The α-β frame is often adopted in PMSM sensorless control to estimate the rotor position [28], and the observability of rotor angle was analyzed in [26], proving that rotor position is observable when the speed is not equal to zero. However, rare studies and research have been carried out to analyze the motor parameter observability in the α-β frame.

Similar to the analysis in the d-q frame, the state function becomes (18) after extending the state vector to motor parameters

$$\frac{d}{dt} i_\alpha = \frac{-R_s}{L_d} i_\alpha - \omega_e \frac{L_d - L_q}{L_d} i_\beta + \frac{1}{L_d} v_\alpha - \frac{1}{L_d} E_\alpha$$

$$\frac{d}{dt} i_\beta = \frac{-R_s}{L_d} i_\beta - \omega_e \frac{L_d - L_q}{L_d} i_\alpha + \frac{1}{L_d} v_\beta - \frac{1}{L_d} E_\beta$$

$$\frac{d}{dt} R_s = 0; \frac{d}{dt} L_d = 0; \frac{d}{dt} L_q = 0; \frac{d}{dt} \psi_f = 0 \tag{18}$$

where

$$E_\alpha = -[(L_d - L_q)(\omega_e i_d - pi_q) + \omega_e \psi_f]\sin\theta_e$$

$$E_\beta = [(L_d - L_q)(\omega_e i_d - pi_q) + \omega_e \psi_f]\cos\theta_e \quad (19)$$

using the theory of parameter observability; let

$$\boldsymbol{x} = \begin{bmatrix} i_\alpha i_\beta R_s L_d L_q \psi_f \end{bmatrix}^T, \boldsymbol{y} = h(\boldsymbol{x}) = \begin{bmatrix} i_\alpha i_\beta \end{bmatrix}^T$$

$$\boldsymbol{u} = \begin{bmatrix} v_\alpha v_\beta \omega_e \theta_e \end{bmatrix}^T \quad (20)$$

$$f(\boldsymbol{x}, \boldsymbol{u}) = \begin{bmatrix} \frac{-R_s}{L_d} i_\alpha - \omega_e \frac{L_d - L_q}{L_d} i_\beta + \frac{1}{L_d} v_\alpha - \frac{1}{L_d} E_\alpha \\ \frac{-R_s}{L_d} i_\beta - \omega_e \frac{L_d - L_q}{L_d} i_\alpha + \frac{1}{L_d} v_\beta - \frac{1}{L_d} E_\beta \\ 0 \\ 0 \\ 0 \\ 0 \end{bmatrix}. \quad (21)$$

Then, according to (6), (7), (20), and (21), the rank of observability matrix $\boldsymbol{O}''_{\text{sub}}$ can be calculated as

$$\text{rank}(\boldsymbol{O}''_{\text{sub}}) = \text{rank} \begin{bmatrix} -i_\alpha & O''_{12} & O''_{13} & \omega_e \sin\theta_e \\ -i_\beta & O''_{22} & O''_{23} & -\omega_e \cos\theta_e \\ O''_{31} & O''_{32} & O''_{33} & O''_{34} \\ O''_{41} & O''_{42} & O''_{43} & O''_{44} \end{bmatrix} \quad (22)$$

where

$$O''_{12} = -\sin\theta_e(pi_q - i_d\omega_e) - i_\beta\omega_e - \frac{1}{L_d}\frac{di_\alpha}{dt}$$

$$O''_{13} = \sin\theta_e(pi_q - i_d\omega_e) + i_\beta\omega_e$$

$$O''_{22} = \cos\theta_e(pi_q - i_d\omega_e) - i_\alpha\omega_e - \frac{1}{L_d}\frac{di_\beta}{dt}$$

$$O''_{23} = -\cos\theta_e(pi_q - i_d\omega_e) + i_\alpha\omega_e$$

$$O''_{31} = R_s i_\alpha + i_\beta\omega_e(L_d - L_q) - L_d\frac{di_\alpha}{dt}$$

$$O''_{32} = R_s O''_{13} - \omega_e(L_d - L_q)O''_{23} - \frac{du_\alpha}{dt} - 2R\frac{di_\alpha}{dt}$$

$$+ \omega_e(L_d - 2L_q)\frac{di_\beta}{dt}$$

$$- \omega_e(E_\beta + \cos\theta_e L_d(pi_q - i_d\omega_e))$$

$$O''_{33} = \omega_e L_d \left(\cos\theta_e(pi_q - i_d\omega_e) + \frac{di_\beta}{dt} \right) - R_s O''_{13}$$

$$- \omega_e(L_d - L_q)O''_{23}$$

$$O''_{34} = \omega_e{}^2\cos\theta_e(2L_d - L_q) - R_s\omega_e\sin\theta_e$$

$$O''_{41} = R_s i_\beta - i_\alpha\omega_e(L_d - L_q) + L_d\frac{di_\beta}{dt}$$

$$O''_{42} = R_s O''_{23} - \omega_e(L_d - L_q)O''_{13} - \frac{du_\beta}{dt} + 2R\frac{di_\beta}{dt}$$

$$- \omega_e(L_d - 2L_q)\frac{di_\alpha}{dt}$$

$$+ \omega_e(E_\alpha - \sin\theta_e L_d(pi_q - i_d\omega_e))$$

$$O''_{43} = \omega_e L_d \left(\sin\theta_e(pi_q - i_d\omega_e) - \frac{di_\alpha}{dt} \right) - R_s O''_{23}$$

$$+ \omega_e(L_d - L_q)O''_{13}$$

$$O''_{44} = \omega_e{}^2\sin\theta_e(2L_d - L_q) + R_s\omega_e\cos\theta_e. \quad (23)$$

Since the matrix in (22) is particularly complex, its determinant can be calculated by resorting to symbolic math toolbox in MATLAB. It can be easily seen that

$$\det(\boldsymbol{O}''_{\text{sub}}) = 0 (\text{if } \omega_e = 0 \text{ or } i_{\alpha\beta} = 0) \quad (24)$$

which means the matrix is not full-rank when the motor speed or currents are zero; the parameters are not observable under the α-β frame in these cases.

III. METHODS OF FULL PARAMETER ESTIMATION

A. RLS Algorithm

RLS is a basic algorithm to estimate weight coefficients. It has been widely used in parameter estimation for its simplicity [29], [30]. Assuming that there is a system with M inputs and that the output is a linear combination of the inputs, in each iteration, the output of the system can be expressed as

$$y(i) = w_1(i)x_1(i) + w_2(i)x_2(i) + \cdots + w_M(i)x_M(i)$$

$$= \boldsymbol{W}(i)^T \boldsymbol{X}(i) \quad (25)$$

where i represents the ith iteration, y is the system output, x_k denotes the kth input, and x_k could not be zero or near to zero; otherwise, its weight coefficient is not able to be estimated. The weight coefficients of system w_k are usually unknown and need to be estimated. An instrumental variable $s(i)$ is introduced

$$s(i) = \hat{w}_1(i)x_1(i) + \hat{w}_2(i)x_2(i) + \cdots + \hat{w}_M(i)x_M(i)$$

$$= \hat{\boldsymbol{W}}(i)^T \boldsymbol{X}(i) \quad (26)$$

where $\hat{w}_k$ is the estimated weight coefficient of the kth input. The error between $s(i)$ and $y(i)$ is defined as $e(i) = y(i) - s(i)$, and a cost function is introduced as

$$J(w) = \frac{1}{2}[y(i) - s(i)]^2. \quad (27)$$

The estimation accuracy is guaranteed when the cost function is minimized. Utilizing the gradient descent algorithm, the updating operation of the estimated weight coefficients can be obtained as

$$\hat{\boldsymbol{W}}(i) = \hat{\boldsymbol{W}}(i-1) + \boldsymbol{K}(i)[y(i) - \hat{\boldsymbol{W}}(i-1)^T \boldsymbol{X}(i)]$$

$$\boldsymbol{K}(i) = \frac{\boldsymbol{P}(i-1)\boldsymbol{X}(i)}{\lambda + \boldsymbol{X}(i)^T \boldsymbol{P}(i-1)\boldsymbol{X}(i)}$$

$$\boldsymbol{P}(i) = [\boldsymbol{I} - \boldsymbol{K}(i)\boldsymbol{X}(i)^T]\boldsymbol{P}(i-1)/\lambda \quad (28)$$

where λ represents the forgetting factor, which can overcome the problem of data saturation; λ is always set between 0.9 and 1. The whole flowchart of the RLS algorithm stated in (28) is shown in Fig. 1.
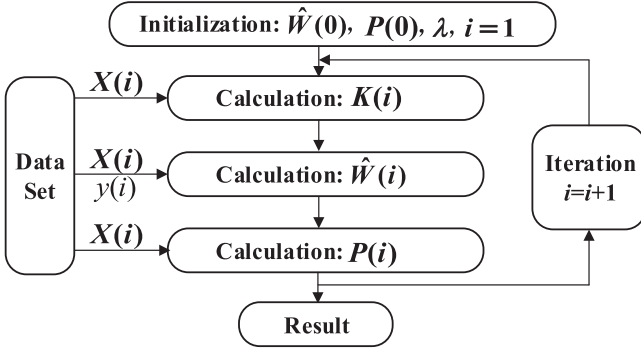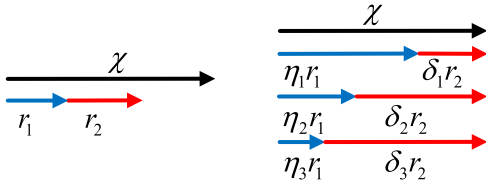
Fig. 1.   Flowchart of the RLS algorithm.

Fig. 2.   System with single input and single output in the *d-q* frame.

Fig. 3.   System with two inputs and single output in the *d-q* frame.

B. RLS in Different Frames

The RLS algorithm cannot be applied to all forms of system (25) to figure out the weight coefficients. In the *d-q* frame, the values of voltages and currents are constant in the steady state. Usually, only one weight coefficient can be estimated in constant frame. For a system simplified from (25), we have

$$\chi = \eta r \tag{29}$$

where r is the single input of the system, χ is the output of the system, and η is the weight coefficient. The input χ and output r are both constant; they can be described in Fig. 2. When both χ and r are given their values, the weight coefficient η can be ascertained with only and real value. If there are two inputs in (29), which can be expressed as

$$\chi = \eta r_1 + \delta r_2 \tag{30}$$

where r_1 and r_2 are the two inputs of system and η and δ are their weight coefficients, respectively. r_1 and r_2 are still constant values; their weight coefficients cannot be defined certainly, which is shown in Fig. 3. There could exist countless possibilities of η and δ such as (η_1, δ_1), (η_2, δ_2), (η_3, δ_3), and so on. In other words, η and δ are not observable. The situation is different in the α-β frame; during the steady state, the voltages and currents are not constant but sinusoidal. In the α-β frame, the system
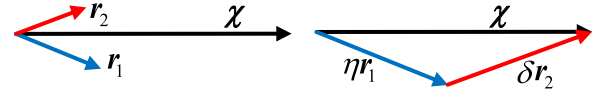
Fig. 4.   System with two inputs and single output in the $\alpha\beta$ frame.
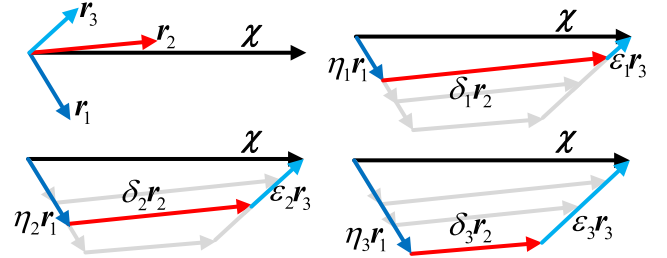
Fig. 5.   System with three inputs and single output in the $\alpha\beta$ frame.

with two inputs and single output can be expressed as

$$\chi = \eta r_1 + \delta r_2 \tag{31}$$

where r_1 and r_2 are the two inputs and χ is the output. All of them are sinusoidal phasors in the α-β frame, and there exist phase differences among them. The relationship of r_1, r_2, and χ is described in Fig. 4. Since the angles of phase differences are fixed in the steady state, η and δ can be identified with only values according to the mathematical triangle theorem. It should be remarked that when there is no phase difference (or with the phase difference of 180°) among r_1, r_2, and χ, the situation becomes what is described in Fig. 3, and there is no way to identify η and δ simultaneously.

When there are three or more inputs in the α-β frame, the system in (31) becomes

$$\chi = \eta r_1 + \delta r_2 + \varepsilon r_3 \tag{32}$$

where r_3 is the third input and ε is the weight coefficient. Likewise, there could exist countless possibilities of η, δ, and ε such as $(\eta_1, \delta_1, \varepsilon_1)$, $(\eta_2, \delta_2, \varepsilon_2)$, $(\eta_3, \delta_3, \varepsilon_3)$, and so on, which is shown in Fig. 5.

Now, it is clear that for each voltage function, only one parameter can be estimated in the *d-q* frame, while two parameters can be estimated in the α-β frame. Both α-β and *d-q* frames have two voltage functions; in the α-β frame, four motor parameters, including stator resistance, *d*-axis and *q*-axis inductances, and flux linkage, can be estimated through two voltage functions.

C. Proposed Method of Full Parameter Estimation

The proposed method of full parameter estimation in the α-β frame can be described as

$$v_\alpha - \hat{W}_{\alpha 2} X_{\alpha 2} = \hat{W}_{\alpha 1} X_{\alpha 1}$$
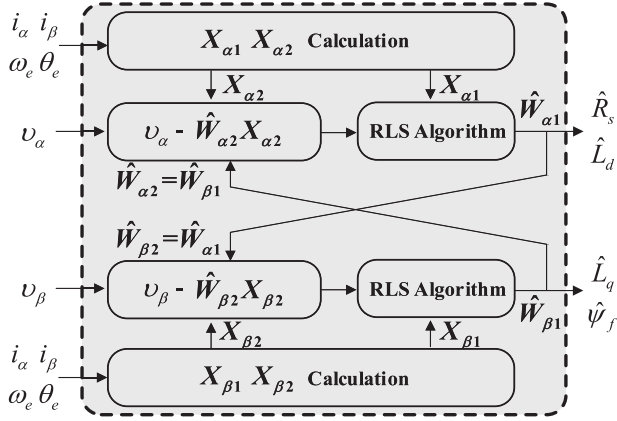$$v_\beta - \hat{W}_{\beta 2} X_{\beta 2} = \hat{W}_{\beta 1} X_{\beta 1} \tag{33}$$

Fig. 6. Proposed full parameter estimation block.

TABLE I
NOMINAL PARAMETERS OF THE TESTED PMSM

Parameters	Value
Type	IPMSM
R_S (Ω)	0.065
L_d (μH)	37.3
L_q (μH)	48.8
ψ_f (Wb)	0.02
Rated Speed (rpm)	1500
Rated Torque (Nm)	5
Vdc (V)	60

Fig. 7. Overall control block of the PMSM.

where

$$\hat{W}_{\alpha 1} = \hat{W}_{\beta 2} = \left[\hat{R}_s \hat{L}_d\right]; \hat{W}_{\alpha 2} = \hat{W}_{\beta 1} = \left[\hat{L}_q \hat{\psi}_f\right]$$

$$X_{\alpha 1} = \begin{bmatrix} i_\alpha \\ \frac{1}{2}pi_\alpha + (\frac{1}{2}pi_\beta - \omega_e i_\alpha)\sin 2\theta_e + (\frac{1}{2}pi_\alpha + \omega_e i_\beta)\cos 2\theta_e \end{bmatrix}$$

$$X_{\alpha 2} = \begin{bmatrix} \frac{1}{2}pi_\alpha - (\frac{1}{2}pi_\beta - \omega_e i_\alpha)\sin 2\theta_e - (\frac{1}{2}pi_\alpha + \omega_e i_\beta)\cos 2\theta_e \\ -\omega_e\sin\theta_e \end{bmatrix}$$

$$X_{\beta 1} = \begin{bmatrix} \frac{1}{2}pi_\beta + (\frac{1}{2}pi_\beta - \omega_e i_\alpha)\cos 2\theta_e - (\frac{1}{2}pi_\alpha + \omega_e i_\beta)\sin 2\theta_e \\ \omega_e\cos\theta_e \end{bmatrix}$$

$$X_{\beta 2} = \begin{bmatrix} i_\beta \\ \frac{1}{2}pi_\beta - (\frac{1}{2}pi_\beta - \omega_e i_\alpha)\cos 2\theta_e + (\frac{1}{2}pi_\alpha + \omega_e i_\beta)\sin 2\theta_e \end{bmatrix}. \quad (34)$$

According to (33), the full parameter estimation can be divided into two procedures: the α-axis voltage function is used to estimate $\hat{R}_s$ and $\hat{L}_d$, while the β-axis voltage function is used to estimate $\hat{L}_q$ and $\hat{\psi}_f$. Fig. 6 shows the whole block of the proposed full parameter estimation. The measurements of i_α, i_β, θ_e, and ω_e are utilized to calculate $X_{\alpha 1}, X_{\alpha 2}, X_{\beta 1}$, and $X_{\beta 2}$ according to (34). In the α-axis voltage function, the value of $\hat{W}_{\alpha 2}$ is needed to calculate the input of the RLS algorithm $v_\alpha - \hat{W}_{\alpha 2}X_{\alpha 2}$; in the proposed method, $\hat{W}_{\alpha 2}$ is from the estimated results $\hat{W}_{\beta 1} = [\hat{L}_q \ \hat{\psi}_f]$ in the β-axis voltage function. After that, the values of $v_\alpha - \hat{W}_{\alpha 2}X_{\alpha 2}$ and $X_{\alpha 1}$ are acquired; $\hat{W}_{\alpha 1}$ can be estimated with the RLS algorithm based on (25)–(28). The same operation is applied to the β-axis voltage function to identify the values of $\hat{W}_{\beta 1}$. In the β-axis voltage function, the value of $\hat{W}_{\beta 2}$ is needed to calculate the input of the RLS algorithm $v_\beta - \hat{W}_{\beta 2}X_{\beta 2}$, and it is from the estimated results $\hat{W}_{\alpha 1} = [\hat{R}_s \ \hat{L}_d]$ in the α-axis voltage function.

In total, it needs to use the RLS algorithm twice to finish one loop of full parameter estimation.

To guarantee the convergence of the proposed method in (33), some conditions should be assured and satisfied: First, as introduced in (31) and Fig. 4, the phase difference of input phasors cannot be zero or 180°. Thus, in (34), the two elements of $X_{\alpha 1}$ cannot have same or inverse phases and neither do the two input elements of $X_{\beta 1}$. Second, the initial values of $\hat{W}_{\alpha 2}$ and

$\hat{W}_{\beta 2}$ could be set as their nominal or adjacent values in order to gain better convergence performance [22].

IV. SIMULATIONS

Simulations based on MATLAB/Simulink for parameter estimation are carried out in this section. The nominal parameters of tested motor in simulation are presented in Table I, and the overall control block is shown in Fig. 7. It should be remarked that the resistance of inverter components must be taken into account in the nominal value of R_s in Table I.

Sometimes, the motor drive hardware is not equipped with phase voltage measurements especially in some situations that the hardware cost is considered. Then, the given reference values of voltages v_α^* and v_β^* could be utilized. Executing the proposed algorithm of full parameter estimation, the simulation results of the interior permanent magnet synchronous motor (IPMSM) in the α-β frame is shown in Fig. 8.

The results in Fig. 8 can prove the effectiveness of the proposed full parameter estimation algorithm in the α-β frame. All of the estimated values of motor parameters are closed to their nominal values in Table I. Actually, in the simulations, the errors between nominal and estimated values are almost zero. The tested motor is running at its rated speed 1500 r/min all the time, but the load added to the motor changes from 0 to 5 N · m at 0.2 s. It can be seen that during the transient state, the change of load has little impact on the estimation of motor parameters. Actually, the increase of load can help to estimate
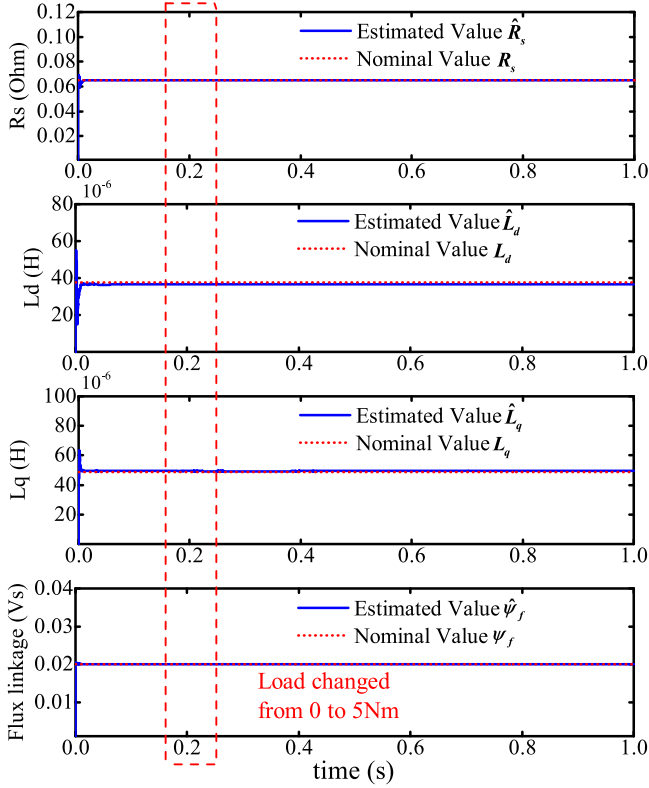
Fig. 8. Simulation results of the IPMSM in the α-β frame.

motor parameters more precisely. When the load is too low, the currents are too small, which makes it a bit difficult to calculate the derivatives of currents. The increase in load can improve the derivatives of currents, the items pi_α and pi_β in (34), which could also make the parameter estimation more accurate.

V. EXPERIMENTAL RESULTS

An experimental system of PMSM control and drive has been set up to implement the algorithms of full parameter estimation that this article depicts in the previous sections, as shown in Fig. 9. The system contains the tested commercial motor, the control and drive board based on the STM32F103 microcontroller, the dynamometer, and other subsidiary equipment. The nominal parameters of the tested PMSM are the same as the values in Table I.

Considering that the frequency of the main interrupt set in STM32F103 is 10 kHz, the frequency of parameter estimation is 1 kHz, which is adequate in most cases. The value of λ used in the experiments is 0.99.

A. Steady State

At the beginning, the motor is running at its rated speed of 1500 r/min and rated torque of 5 N · m to verify the effectiveness of the proposed algorithm in the steady state. Fig. 10 demonstrates the experimental results using the proposed estimation method in the α-β frame. Similar to the simulations, it can be clearly seen that all of the estimated motor parameters can
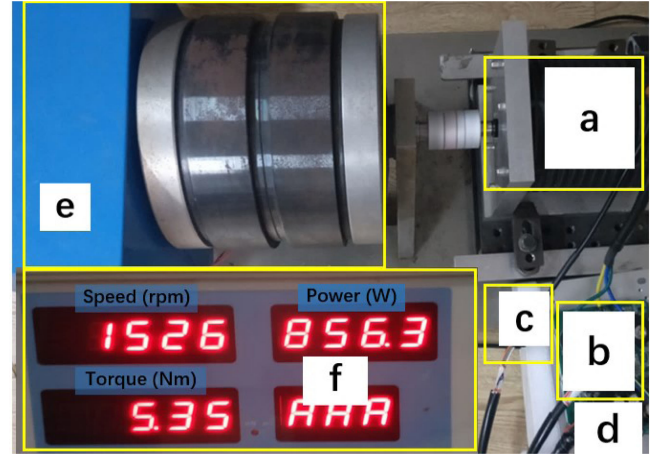

Fig. 9. Experiment Rig. (a) Commercial PMSM. (b) STM32F103 microcontroller and motor drive board. (c) Encoder. (d) DC power supply. (e) Dynamometer. (f) Front panel of the dynamometer.
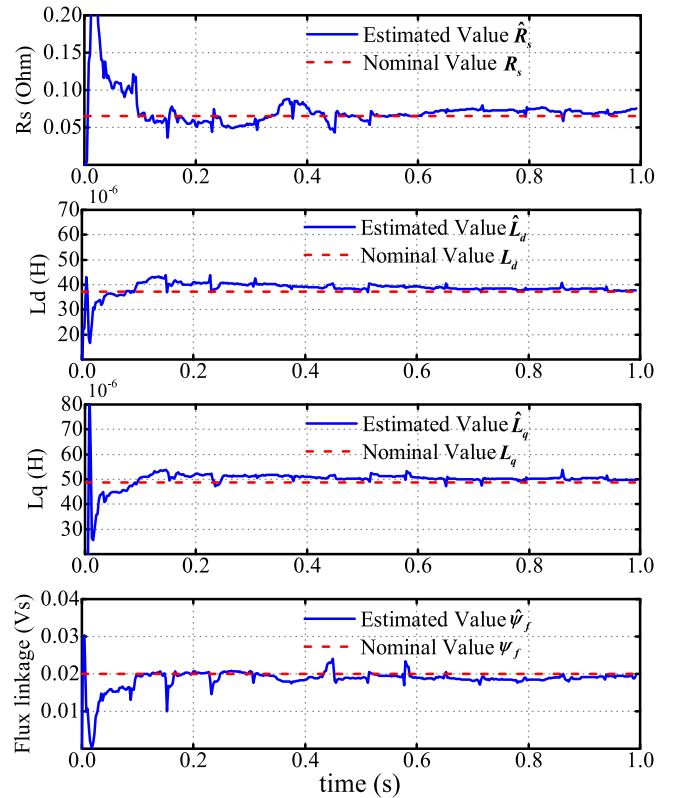
Fig. 10. Experimental results of the proposed estimation method.

converge to their nominal values quickly. Table II presents the percentage error of nominal and estimated parameters. The estimated stator resistance $\hat{R}_s$ is about 0.068 Ω, the estimated d-axis inductance $\hat{L}_d$ is about 38.0 μH, and the estimated q-axis inductance $\hat{L}_q$ is approximately 50.0 μH; the estimated flux linkage is around 0.0195 Wb, and the errors are acceptable.

In order to know the impact of rotation speed and current value on the accuracy of the estimated parameters, the results of different torques and different speeds are shown in Tables III

TABLE II
PERCENTAGE ERROR OF NOMINAL AND ESTIMATED PARAMETERS

Parameters	Nominal Value	Estimated Value	Error(%)
R_s (Ω)	0.065	0.068	4.61
L_d (μH)	37.3	38.0	1.87
L_q (μH)	48.8	50.0	2.45
ψ_f (Wb)	0.02	0.0195	-2.5

TABLE III
PARAMETER ESTIMATION RESULTS OF DIFFERENT TORQUES (1500 R/MIN)

Torque	0 Nm	1 Nm	2 Nm	3 Nm	4 Nm	5 Nm
i_α (A, RMS)	2.8	8.4	14.1	18.4	22.6	27.5
R_s (Ω)	0.050	0.055	0.061	0.066	0.067	0.068
L_d (μH)	48.5	43.2	36.8	37.5	38.5	38.0
L_q (μH)	57.5	52.0	49.5	50.5	50.0	50.0
ψ_f (Wb)	0.0180	0.0195	0.0205	0.0200	0.0195	0.0195

TABLE IV
PARAMETER ESTIMATION RESULTS OF DIFFERENT SPEEDS (5 N · M)

Speed	0 rpm	100 rpm	500 rpm	1000 rpm	1500 rpm
R_s (Ω)	-	0.060	0.065	0.068	0.068
L_d (μH)	-	36.5	38.5	38.0	38.0
L_q (μH)	-	47.0	48.5	50.5	50.0
ψ_f (Wb)	-	0.0250	0.0210	0.0200	0.0195

Fig. 11. Experimental results using the algorithm with two different convergence rates.

and IV correspondingly. It can be seen from Table III that the estimated results of motor parameters are satisfactory when the load torque is heavier than 1 N · m. The estimated results of *d*- and *q*-axis inductances are not very good with low or no load since the currents are small, and it is hard to measure the currents precisely. From Table IV, the results are acceptable in the medium and high speeds. When the speed is too low, the flux linkage ψ_f cannot be estimated precisely because the back electromotive force is too small. It should be noted that when the speed is zero, there is no way to estimate any parameters according to (24).

To further assess the merits of estimation methods proposed in this article, a contrastive study with other existing algorithms is carried out. For instance, in [16], the algorithm of parameter estimation is still conducted in the *d-q* frame, but it possesses two-time-scale estimation algorithms with different convergence rates.

1) *Fast convergence rate to estimate $\hat{L}_d$ and $\hat{L}_q$:*

According to the PMSM model in the *d-q* frame (1), we have

$$v_d - \hat{R}_s i_d - \hat{L}_d p i_d = -\hat{L}_q \omega_e i_q$$
$$v_q - \hat{R}_s i_q - \hat{L}_q p i_q - \omega_e \hat{\psi}_f = \omega_e \hat{L}_d i_d. \quad (35)$$

The items of pi_d and pi_q can be ignored in the steady state.

2) *Slow convergence rate to estimate $\hat{R}_s$ and $\hat{\psi}_f$:*

$$v_d - \hat{L}_d p i_d + \hat{L}_q \omega_e i_q = \hat{R}_s i_d$$
$$v_q - \hat{L}_q p i_q - \hat{L}_d \omega_e i_d = \hat{R}_s i_q + \omega_e \hat{\psi}_f. \quad (36)$$

Each *d*-axis or *q*-axis voltage functions in (35) and (36) can be used to estimate one motor parameter. Therefore, in order to

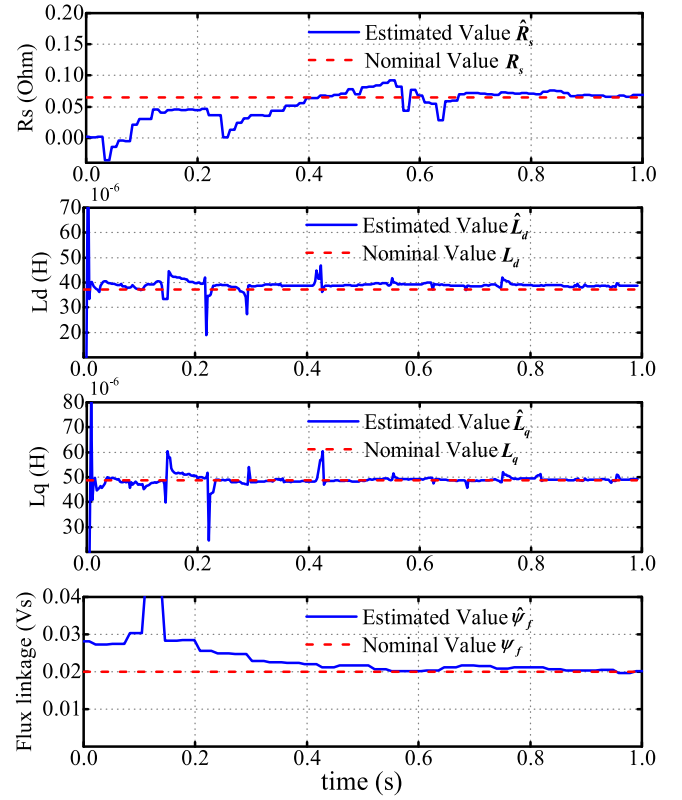estimate the full motor parameters, the RLS algorithm must be implemented for four times, which may increase the computer complexity and consume more time.

The experimental results of this algorithm in the convergence process are presented in Fig. 11. The speed of the motor is still maintained at its rated speed 1500 r/min; the torque is also 5 N · m. Using the algorithm in the *d-q* frame, it takes more time to converge to the nominal values. In Fig. 11, it takes approximately more than 0.4 s to get to the nominal value of R_s and 0.5 s to converge to the real value of ψ_f. In the α-β frame, apparently, it takes less time, as shown in Fig. 10, about 0.1 s to converge to the nominal value of R_s and 0.15 s to converge to the real value of ψ_f. The roughly 0.3-s improvement of convergence time is crucial at times. For instance, some control strategies are rather sensitive to the motor parameters such as deadbeat and predictive current control [31]. Also, the proposed method can be applied to fault diagnosis such as demagnetization [32].

Moreover, Table V states the comparison of different methods on the same hardware, including the method in the α-β frame, the approach in the *d-q* frame, and the Kalman filter [33], [34]. The items of dataset, computation cost, and advantages and disadvantages are elaborated. It should be remarked that the quantities used in the parameter estimation algorithm such as i_α, i_β, v_α, v_β, $\sin\theta_e$, and $\cos\theta_e$ (generally lookup table is applied to calculate $\sin\theta_e$ and $\cos\theta_e$) are preprepared in the field-oriented control of the PMSM, which will not cost extra computational time of the parameter estimation algorithm. Then, the quantities

TABLE V
COMPARISON OF DIFFERENT METHODS

|	Proposed method in α-β frame	The method in d-q frame	Kalman Filter
Data Set	currents,voltages rotor position	currents,voltages rotor position	currents,voltages rotor position
Computation Cost of One Iteration	96μs	125μs	210μs
Number of Estimated Parameters	4	4	1 (ψ_f)
Advantages	1) full parameters can be estimated with α-β voltage functions 2) less computation and convergence time	simple theoretical derivation and implementation	consider the noise probability distribution and enable to reject measurement noise
Disadvantages	1) initial sensitivity 2) perform not well with low speed or light load	1) only two parameters can be estimated with d-q voltage functions and have to use 4 RLS algorithms to finish full parameters estimation 2) initial sensitivity 3) perform not well with low speed or light load	high computational burden and therefore Kalman Filter is often utilized to estimate one or two parameters
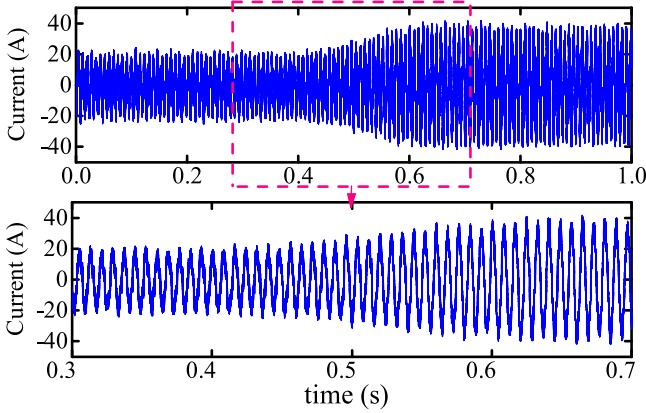
Fig. 12. α-axis current in the transient process.

such as $\sin 2\theta_e$ and $\cos 2\theta_e$ utilized in the parameter estimation algorithm could be calculated from $\sin\theta_e$ and $\cos\theta_e$ through simple operators. From Table V, the computational cost in the α-β frame is less than in the d-q frame. In addition, both methods in d-q and α-β frames are sensitive to θ_e; hence, it is required to get the precise rotor position.

B. Transient Performance

To verify the performance of the proposed algorithm in the transient state, the torque of motor is changed from 2 to 5 N · m at 0.4 s, and the speed is still maintained as 1500 r/min; Figs. 12 and 13 show the results during the transient state. Fig. 12 presents the α-axis current when the torque is changed from 2 to 5 N · m. In Fig. 13, it can be seen that although there are some disturbances when the torque changes at 0.4 s, the estimated results can quickly converge to their nominal values. The increase in current will improve the derivative of currents, which can help to estimate the motor parameters more precisely. For instance, the stator resistance and the d-axis inductance are closer to their nominal values when the torque is increasing.
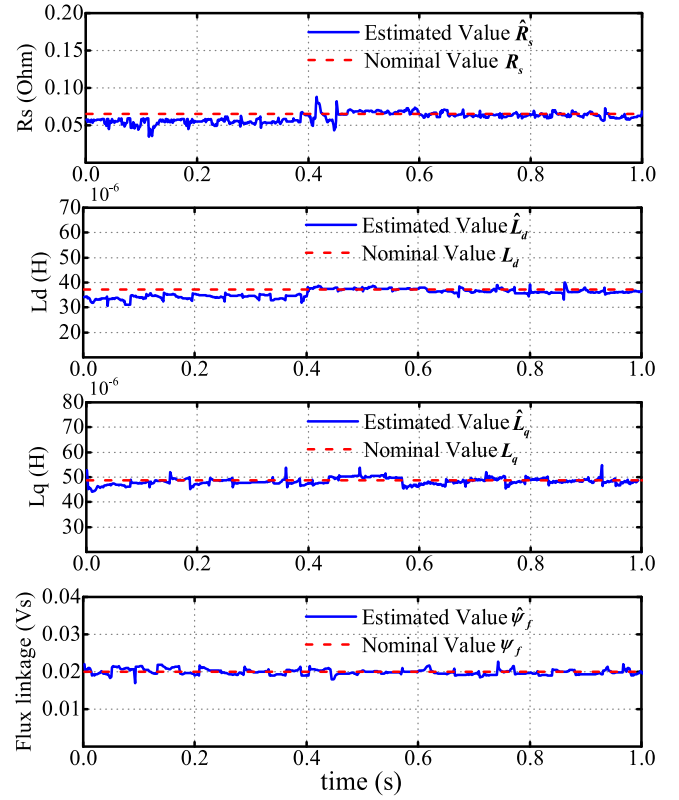

Fig. 13.   Experimental results in the transient state.

VI. CONCLUSION

The main purpose of this article was to propose a novel full parameter estimation method. The parameter observability in different frames was first figured out. In addition, it was found that only one motor parameter can be identified using each of the voltage functions in the d-q frame, while two motor parameters can be estimated in the α-β frame. A feasible approach of full parameter estimation based on the α-β frame and RLS was illustrated. Simulation and experiment results manifested the effectiveness of the proposed full parameter estimation algorithms in the α-β frame during both steady and transient states. Comparisons with other existing algorithms proved that the proposed method has the advantages of faster convergence rate, less computational cost, and high accuracy.

REFERENCES

[1] G. Pellegrino, A. Vagati, P. Guglielmi, and B. Boazzo, "Performance comparison between surface-mounted and interior PM motor drives for electric vehicle application," *IEEE Trans. Ind. Electron.*, vol. 59, no. 2, pp. 803–811, Feb. 2012.

[2] F. Fernandez-Bernal, A. Garcia-Cerrada, and R. Faure, "Determination of parameters in interior permanent-magnet synchronous motors with iron losses without torque measurement," *IEEE Trans. Ind. Appl.*, vol. 37, no. 5, pp. 1265–1272, Sep./Oct. 2001.

[3] P. H. Mellor, M. A. Al-Taee, and K. J. Binns, "Open loop stability characteristics of synchronous drive incorporating high field permanent magnet motor," in *Proc. Inst. Elect. Eng.—Elect. Power Appl.*, vol. 138, no. 4, pp. 175–184, 1991.

[4] K. Liu and Z. Q. Zhu, "Online estimation of the rotor flux linkage and voltage-source inverter nonlinearity in permanent magnet synchronous machine drives," *IEEE Trans. Power Electron.*, vol. 29, no. 1, pp. 418–427, Jan. 2014.

[5] C. C. Hwang and Y. H. Cho, "Effects of leakage flux on magnetic fields of interior permanent magnet synchronous motors," *IEEE Trans. Magn.*, vol. 37, no. 4, pp. 3021–3024, Jul. 2001.

[6] L. Tao, Q. Chen, Y. Luo, and Y. Nan, "Adaptive parameter identification and control for servo system with input saturation," in *Proc. 9th Int. Conf. Model., Identification Control*, 2017, pp. 652–657.

[7] E. Samygina, M. Tiapkin, L. Rassudov, and A. Balkovoi, "Extended algorithm of electrical parameters identification via frequency response analysis," in *Proc. 26th Int. Workshop Elect. Drives: Improvement Efficiency Electr. Drives*, 2019, pp. 1–4.

[8] S. Gao, H. Dong, B. Ning, T. Tang, and Y. Li, "Nonlinear mapping-based feedback technique of dynamic surface control for the chaotic PMSM using neural approximation and parameter identification," *IET Control Theory Appl.*, vol. 12, no. 6, pp. 819–827, 2018.

[9] D. Puangdownreong, S. Hlungnamtip, C. Thammarat, and A. Nawikavatan, "Application of flower pollination algorithm to parameter identification of dc motor model," in *Proc. Int. Elect. Eng. Congr.*, 2017, pp. 1–4.

[10] A. Avdeev and O. Osipov, "PMSM identification using genetic algorithm," in *Proc. 26th Int. Workshop Elect. Drives: Improvement Efficiency Electr. Drives*, 2019, pp. 1–4.

[11] S. Nalakath, M. Preindl, and A. Emadi, "Online multi-parameter estimation of interior permanent magnet motor drives with finite control set model predictive control," *IET Electr. Power Appl.*, vol. 11, no. 5, pp. 944–951, 2017.

[12] G. Feng, C. Lai, K. Mukherjee, and N. C. Kar, "Current injection-based online parameter and VSI nonlinearity estimation for PMSM drives using current and voltage DC components," *IEEE Trans. Transp. Electrific.*, vol. 2, no. 2, pp. 119–128, Jun. 2016.

[13] M. S. Rafaq and J. Jung, "A comprehensive review of state-of-the-art parameter estimation techniques for permanent magnet synchronous motors in wide speed range," *IEEE Trans. Ind. Informat.*, vol. 16, no. 7, pp. 4747–4758, Jul. 2020.

[14] Y. Inoue, Y. Kawaguchi, S. Morimoto, and M. Sanada, "Performance improvement of sensorless IPMSM drives in a low-speed region using online parameter identification," *IEEE Trans. Ind. Appl.*, vol. 47, no. 2, pp. 798–804, Mar./Apr. 2011.

[15] L. Yan, D. Zhang, Z. Bai, P. Ye, and C. Zhang, "Online multi-parameter identification of long-mover permanent magnet linear motor," in *Proc. 22nd Int. Conf. Elect. Mach. Syst.*, 2019, pp. 1–5.

[16] D. Q. Dang, M. S. Rafaq, H. H. Choi, and J. Jung, "Online parameter estimation technique for adaptive control applications of interior pm synchronous motor drives," *IEEE Trans. Ind. Electron.*, vol. 63, no. 3, pp. 1438–1449, Mar. 2016.

[17] S. Ichikawa, M. Tomita, S. Doki, and S. Okuma, "Sensorless control of permanent-magnet synchronous motors using online parameter identification based on system identification theory," *IEEE Trans. Ind. Electron.*, vol. 53, no. 2, pp. 363–372, Apr. 2006.

[18] J. Zhou, K. Huang, S. Huang, S. Liu, H. Zhao, and M. Shen, "Inductance parameter identification method of permanent magnet synchronous motor based on the HF rotating square wave voltage injection," in *Proc. 22nd Int. Conf. Elect. Mach. Syst.*, 2019, pp. 1–4.

[19] G. Feng, C. Lai, and N. C. Kar, "Particle-filter-based magnet flux linkage estimation for PMSM magnet condition monitoring using harmonics in machine speed," *IEEE Trans. Ind. Informat.*, vol. 13, no. 3, pp. 1280–1290, Jun. 2017.

[20] G. Feng, C. Lai, K. Mukherjee, and N. C. Kar, "Online PMSM magnet flux-linkage estimation for rotor magnet condition monitoring using measured speed harmonics," *IEEE Trans. Ind. Appl.*, vol. 53, no. 3, pp. 2786–2794, May/Jun. 2017.

[21] K. Choi, Y. Kim, K. Kim, and S. Kim, "Using the stator current ripple model for real-time estimation of full parameters of a permanent magnet synchronous motor," *IEEE Access*, vol. 7, pp. 33 369–33379, 2019.

[22] S. J. Underwood and I. Husain, "Online parameter estimation and adaptive control of permanent-magnet synchronous machines," *IEEE Trans. Ind. Electron.*, vol. 57, no. 7, pp. 2435–2443, Jul. 2010.

[23] K. Liu, J. Feng, S. Guo, L. Xiao, and Z. Q. Zhu, "Improved position offset based parameter determination of permanent magnet synchronous machines under different load conditions," *IET Elect. Power Appl.*, vol. 11, no. 4, pp. 603–612, 2017.

[24] R. Hermann and A. Krener, "Nonlinear controllability and observability," *IEEE Trans. Autom. Control*, vol. 22, no. 5, pp. 728–740, Oct. 1977.

[25] M. Koteich, A. Maloum, G. Duc, and G. Sandou, "Discussion on "AC drive observability analysis"," *IEEE Trans. Ind. Electron.*, vol. 62, no. 11, pp. 7224–7225, Nov. 2015.

[26] P. Vaclavek, P. Blaha, and I. Herman, "AC drive observability analysis," *IEEE Trans. Ind. Electron.*, vol. 60, no. 8, pp. 3047–3059, Aug. 2013.

[27] T. Boileau, N. Leboeuf, B. Nahid-Mobarakeh, and F. Meibody-Tabar, "Online identification of PMSM parameters: Parameter identifiability and estimator comparative study," *IEEE Trans. Ind. Appl.*, vol. 47, no. 4, pp. 1944–1957, Jul./Aug. 2011.

[28] Z. Qiao, T. Shi, Y. Wang, Y. Yan, C. Xia, and X. He, "New sliding-mode observer for position sensorless control of permanent-magnet synchronous motor," *IEEE Trans. Ind. Electron.*, vol. 60, no. 2, pp. 710–719, Feb. 2013.

[29] M. S. Rafaq, F. Mwasilu, J. Kim, H. H. Choi, and J. Jung, "Online parameter identification for model-based sensorless control of interior permanent magnet synchronous machine," *IEEE Trans. Power Electron.*, vol. 32, no. 6, pp. 4631–4643, Jun. 2017.

[30] H. Lu, Y. Wang, Y. Yuan, J. Zheng, J. Hu, and X. Qin, "Online identification for permanent magnet synchronous motor based on recursive fixed memory least square method under steady state," in *Proc. 36th Chin. Control Conf.*, 2017, pp. 4824–4829.

[31] S. Decker, J. Richter, and M. Braun, "Predictive current control and online parameter identification of interior permanent magnet synchronous machines," in *Proc. 18th Eur. Conf. Power Electron. Appl.*, 2016, pp. 1–10.

[32] Z. Ullah, S. Lee, M. R. Siddiqi, and J. Hur, "Online diagnosis and severity estimation of partial and uniform irreversible demagnetization fault in interior permanent magnet synchronous motor," in *Proc. IEEE Energy Convers. Congr. Expo.*, 2019, pp. 1682–1686.

[33] F. Mwasilu and J. Jung, "Enhanced fault-tolerant control of interior PMSMs based on an adaptive EKF for EV traction applications," *IEEE Trans. Power Electron.*, vol. 31, no. 8, pp. 5746–5758, Aug. 2016.

[34] F. Auger, M. Hilairet, J. M. Guerrero, E. Monmasson, T. Orlowska-Kowalska, and S. Katsura, "Industrial applications of the Kalman filter: A review," *IEEE Trans. Ind. Electron.*, vol. 60, no. 12, pp. 5458–5471, Dec. 2013.

Yelong Yu was born in Zhejiang, China, in 1995. He received the B.Eng. degree in electrical engineering in 2018 from Zhejiang University, Hangzhou, China, where he is currently working toward the Ph.D. degree in electrical engineering.

His research interests include the motor drive and control, and demagnetization fault diagnosis for permanent magnet synchronous motors.

Xiaoyan Huang (Member, IEEE) received the B.E. degree in control measurement techniques and instrumentation from Zhejiang University, Hangzhou, China, in 2003, and the Ph.D. degree in electrical machines and drives from the University of Nottingham, Nottingham, U.K., in 2008.

From 2008 to 2009, she was a Research Fellow with the University of Nottingham. She is currently a Professor with the College of Electrical Engineering, Zhejiang University, where she is working on electrical machines and drives. Her research interests include permanent magnet machines and drives for aerospace and traction applications and generator systems for urban networks.

Zhaokai Li was born in Lishui, China, in 1993. He received the B.S. and Ph.D. degrees in electrical engineering from Zhejiang University, Hangzhou, China, in 2015 and 2020, respectively.

He is currently a Postdoctoral Researcher with Zhejiang University. His major research interests include the analytical modeling of permanent magnet synchronous motors and iron loss analysis.
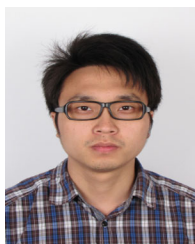
Min Wu received the B.Eng. and M.Sc. degrees in electrical engineering from Zhejiang University, Hangzhou, China, in 2013 and 2017, respectively.

He is currently an Experimental Engineer with the College of Electrical Engineering, Zhejiang University. His research interests include brushless dc motor and permanent magnet machine drives.

Tingna Shi (Member, IEEE) was born in Yuyao, China, in 1969. She received the B.S. and M.S. degrees from Zhejiang University, Hangzhou, China, in 1991 and 1996, respectively, and the Ph.D. degree from Tianjin University, Tianjin, China, in 2009, all in electrical engineering.

She is currently a Professor with the College of Electrical Engineering, Zhejiang University. Her current research interests include electrical machines and their control systems, power electronics, and electric drives.

Yanfei Cao received the B.S. degree in automation from the Hebei University of Technology, Tianjin, China, in 2013, and the M.S. and Ph.D. degrees in control science and engineering from Tianjin University, Tianjin, in 2019.

She is currently a Postdoctoral Researcher with the College of Electrical Engineering, Zhejiang University, Hangzhou, China. Her research interests include electrical machines, motor drives, and power electronics.

Geng Yang (Member, IEEE) received the B.Sc. and M.Sc. degrees in control measurement techniques and instrumentation from the College of Biomedical Engineering and Instrument Science, Zhejiang University, Hangzhou, China, in 2003 and 2006, respectively, and the Ph.D. degree in electronic and computer systems from the KTH Royal Institute of Technology, Stockholm, Sweden, in 2013.

He is currently a Research Professor with the School of Mechanical Engineering, Zhejiang University. He developed low-power low-noise bioelectric system-on-chip sensors for m-health. His research interests include flexible and stretchable electronics, mixed-mode IC design, low-power biomedical microsystem, wearable biodevices, human–computer interface, human–robot interaction, intelligent sensors, and Internet of things for healthcare.

Feng Niu (Member, IEEE) was born in Hebei, China, in 1986. He received the B.S. and Ph.D. degrees in electrical engineering from the Hebei University of Technology, Tianjin, China, in 2009 and 2015, respectively.

From 2012 to 2014, he was a Research Fellow with the Electrical Machines and Drives Laboratory, Michigan State University, East Lansing, MI, USA. From 2016 to 2018, he was a Postdoctoral Research Fellow with the College of Electrical Engineering, Zhejiang University, Hangzhou, China. He is currently a Professor with the School of Electrical Engineering, Hebei University of Technology. He has authored or coauthored more than 50 technical articles. His current research interests include motor system and control and intelligent electrical equipment.